Isothermal Crystallization and Spherulite Structure of Partially Miscible Polypropylene–Linear Low-Density Polyethylene Blends

JUN LI,[1] ROBERT A. SHANKS,[1] YU LONG[2]

[1] Department of Applied Chemistry, RMIT University, Melbourne, Victoria, Australia

2 CSIRO Manufacturing Science and Technology, Clayton, Victoria, Australia

Received 29 August 2000; accepted 11 December 2000

ABSTRACT: Polypropylene (PP) was blended with a linear low-density polyethylene (LLDPE, containing 5% hexene comonomer) over a composition range of 10–90% of PP. The crystallization and morphology of the PP–LLDPE blends were studied by differential scanning calorimetry (DSC), polarized optical microscopy with a hot stage (HSOM), and scanning electron microscopy (SEM). In particular, the isothermal crystallization of PP in molten LLDPE was investigated. It was observed that the crystallization and melting behavior of PP and LLDPE changed in the blends, indicating that there was some degree of miscibility between the PP and the LLDPE. A depression of the equilibrium melting temperature (T_m^0) of PP in the blends with no more than 15% of PP confirmed that PP was miscible with LLDPE at and below 15% of PP. In addition, a drastic decrease in T_m^0 from the 25% PP blend to the 20% blend led us to conclude that the miscible behavior between PP and LLDPE became favorable at a PP concentration of 20%. The optical microscopic images showed that, in the blends with 10 and 15% of PP, the PP crystallized as open-armed diffuse spherulites, similar to those in the miscible blends. In contrast, the PP crystallized in a phase-separated matrix or droplets with more than 25% of PP, when obvious phase separation occurred. The SEM image revealed that the PP lamella was able to penetrate the PP and LLDPE phase boundary and grow in the LLDPE phase. The above results displayed that the PP dissolved in the LLDPE, and, particularly, when the PP concentration was below 20%, the dissolution was substantial. J Appl Polym Sci 82: 628–639, 2001

Key words: polypropylene–polyethylene blends; miscibility; crystallization; spherulites

INTRODUCTION

While polypropylene (PP) and polyethylene (PE) are compatible polymers, there have been debates on their miscibility. The miscibility of PP–PE blends depends on the type of materials and their compositions in the blends.

Phase separation was detected in PP and linear PE (high-density polyethylene, HDPE) melts using light microscopy,[1,2] scanning electron microscopy (SEM),[1] neutron scattering,[3,4] and transmission electron microscopy (TEM).[5] However, Blom et al.[6] recently reported that HDPE was able to penetrate the PP phase sufficiently at low HDPE concentrations to reduce the number and size of high segment density

Correspondence to: J. Li, Department of Applied Chemistry, RMIT University, G.P.O. Box 2476V, Melbourne, Victoria, 3001 Australia (jun.li@rmit.edu.au).

Journal of Applied Polymer Science, Vol. 82, 628–639 (2001)

regions, thereby delaying the nucleation and subsequent crystallization of the PP phase. They concluded that there was a certain degree of interaction between PP and HDPE at HDPE concentrations below 20%.

PP was also found to be immiscible with long-chain-branched PE (low-density polyethylene, LDPE), which was observed by TEM.[7] However, another study on a PP–LDPE blend showed that a small addition of LDPE (10%) caused a depression of the spherulite growth rate of PP and increased the chain-folding energy in PP crystallization.[8] This was interpreted as partial miscibility of PP and LDPE in the melt.

In the case of PP and linear low-density PE (LLDPE) blends, both polymers are linear-chain hydrocarbons with no long chain branching, providing structural similarity. A more miscible behavior between them is therefore expected. The compatibility in the tensile and impact properties of these blends was reported by various authors.[9–16] Dumoulin et al.[9–12] studied the blends in the solid state by differential scanning calorimetry (DSC) and dynamic mechanical thermal analysis (DMTA) and investigated the mechanical properties as well as the melt rheology. The results showed that the blends containing a small proportion of LLDPE (below 5%) was miscible. In contrast, Hill and coworkers[17] studied PP–LLDPE blends by TEM on samples quenched from 190°C and found that there was liquid–liquid phase separation in the PP and LLDPE blends at 190°C with between 1 and 99% of PP. Recently, through a TEM study, Dong et al.[18] found that a fraction of PP dissolved in LLDPE although phase separation was obvious.

Complete miscibility was reported for PP with ethylene–olefin copolymers containing 50 mol % or more butene or hexene comonomers,[19–21] while 33 mol % hexene was still not enough to provide complete miscibility. This led us to think that smaller proportions of a comonomer in the copolymers may provide miscibility for blends in a limited composition and temperature range.

We previously reported[22–24] that PP dissolved in LLDPE (containing 5% of the hexene comonomer) at a PP composition of 20% and at temperatures above the crystallization temperature of LLDPE. In this article, the effect of the composition ratio on the crystallization and morphology of PP and LLDPE was studied. The miscibility of PP and LLDPE will be discussed.

EXPERIMENTAL

Materials and Blend Preparation

An isotactic PP (homopolymer, MFI = 28 g [10 min]$^{-1}$ at 230°C and 2.16 kg load) was blended with an LLDPE (5 mol % hexene copolymer, MFI = 1 g [10 min]$^{-1}$ at 190°C and 2.16 kg load) over a composition range of 10–90% of PP. The blends were mixed in an Axon BX-12 single-screw extruder with a screw diameter of 12.5 mm and length-to-diameter ratio of 26:1, operating with a screw speed of 80 rpm. The temperatures for the feeding zone, melting zone, compression zone, and die were 170, 200, 200, and 180°C, respectively. The blends were extruded with a standard four-hole die as strands and pelletized before sampling.

Differential Scanning Calorimetry (DSC)

A Perkin–Elmer DSC-7 was used to analyze the thermal properties and overall crystallization kinetics of the PP. Crystallization and melting temperature measurements were performed by melting the sample at 200°C for 2 min followed by cooling to 40°C and subsequent reheating to 20°C. A program rate of 10°C min^{-1} was used. For the isothermal crystallization, samples were first melted at 200°C for 5 min and quenched to a temperature 20–30°C higher than the chosen isothermal crystallization temperature (T_c) and held at this temperature for 1 min and then cooled at 50°C min^{-1} to the isothermal crystallization temperature. This two-step quenching program was used to prevent the instrument overshooting the T_c. The selected isothermal crystallization temperatures were between 122 and 130°C. Samples were kept at these temperatures for designated times to allow the PP to crystallize completely. The heat evolved during the isothermal crystallization (ΔH_c) was recorded as a function of time. The crystalline conversion (X_t) at a constant temperature is related to the ratio of heat evolved at time, t, and at infinite time, t_∞, according to the equation

$$X_t = Q_t/Q_\infty = \int_0^t (dH/dt)/\int_0^\infty (dH/dt)\, dt \quad (1)$$

where dH/dt is the rate of heat evolution. The crystallization kinetics can be studied by DSC under isothermal crystallization conditions. Such

isothermal crystallization is generally analyzed using the Avrami equation[25]

$$\ln\{-\ln[1 - X(t, T)]\} = \ln k(T) + n \ln t \quad (2)$$

where *X(t,T)* is the volume fraction of crystalline material at time, *t,* and isothermal crystallization temperature, *T*; *n* is the Avrami exponent which is related to nucleation type and crystal-growth geometry; and the crystallization rate coefficient, *k*, is a parameter of crystallization growth rate and related to the nucleation type, crystal-growth geometry, and crystallization temperature.

The Avrami exponent (*n*, slope of the straight line) and the crystallization rate coefficient (*k*, intersection with the *y* axis) were calculated from a plot of ln[−ln (1 − *X*)] versus ln *t*. Based on these two values, $t_{1/2}$, which is a measure of the crystallization rate, can be obtained from the equation

$$t_{1/2} = \ln 2/(k^{1/n}) \quad (3)$$

After isothermal crystallization, the samples were heated to 200°C at a scanning rate of 10°C min_{-1}. The melting temperatures (T_m) of PP were measured. The equilibrium melting temperature (T_m^0) can be obtained from the Hoffman–Weeks equation

$$T_m = T_m^0/(1 - 1/\gamma) + T_c/\gamma \quad (4)$$

in which γ is the lamellar thickness. In plotting the experimental melting temperature versus the isothermal crystallization temperature, the extrapolation to $T_m = T_c$ is the equilibrium melting temperature.

Hot-stage Optical Microscopy (HSOM)

A Nikon Labophot II microscope with polarized light and equipped with a Mettler FP90 hot stage was used to study the morphology and crystallization of the blends. Images were captured using a Sony video camera and video monitor connected to a computer with IPLab image analysis software. Specimens of 20-μm thickness were prepared with a microtome. The films were heated between glass slides and coverslips in the hot stage to 200°C for 5 min prior to rapid cooling (20°C min^{-1}) to isothermal crystallization temperatures between 124 and 130°C. After a time long enough for the PP to crystallize completely, the glass slides were taken out of the hot stage and let cool naturally.

Measurement of Spherulite Growth Rate

Images of PP spherulites were recorded at appropriate intervals of time according to the growth rate of the spherulites. The area of the spherulites was measured by using IPLab software. Based on the area of the spherulites, two methods can be used to measure the spherulite growth rate. One method is from the slope of the plots of individual radii versus time, and the other is from the slope of average radius versus time. The individual spherulite growth rate, $\dot{g}$, is determined by measuring the area of a randomly chosen spherulite:

$$\dot{g} = \dot{s}\frac{1}{2\sqrt{\pi s}} \quad (5)$$

in which $\dot{s} = ds/dt$ and *s* is the area of the measured spherulite. The individual growth, $\dot{g}$, is determined by plotting $\sqrt{s/\pi}$ versus *t*. The average growth rate, *G*, is determined by measuring the crystallized fraction and the number of the spherulites in the field of view, then plotting $\sqrt{X/n\pi}$ versus *t*.

Errors brought by impinged spherulites were moderated in the calculation. As the program only considers spherulites as particles, with broken boundaries as one, it may falsely consider impinged spherulites as one particle. In this case, joined particles were separated manually by drawing lines on the computer screen. Another way to remove these errors is to set a threshold value to remove all clearly impossible data. For example, the size of the PP spherulite in our study is less than 100 μm across. Any particles that are greater than 100 μm could be impinged spherulites and will be recognized by the computer and be removed. It is noted that the scale has to be properly calibrated when calculating the spherulite radius and growth rate.

Scanning Electron Microscopy (SEM)

The films crystallized in the HSOM were taken carefully out of the glass slides and coverslips and then etched for 1 h in a solution of 1% wt/vol potassium permanganate with a mixture of 10 vol concentrated sulfuric acid and 4 vol of orthophosphoric acid as a solvent. After being vacuum-dried, the films were gold-coated in an SPI sputter coater. To avoid overheating, the coating was

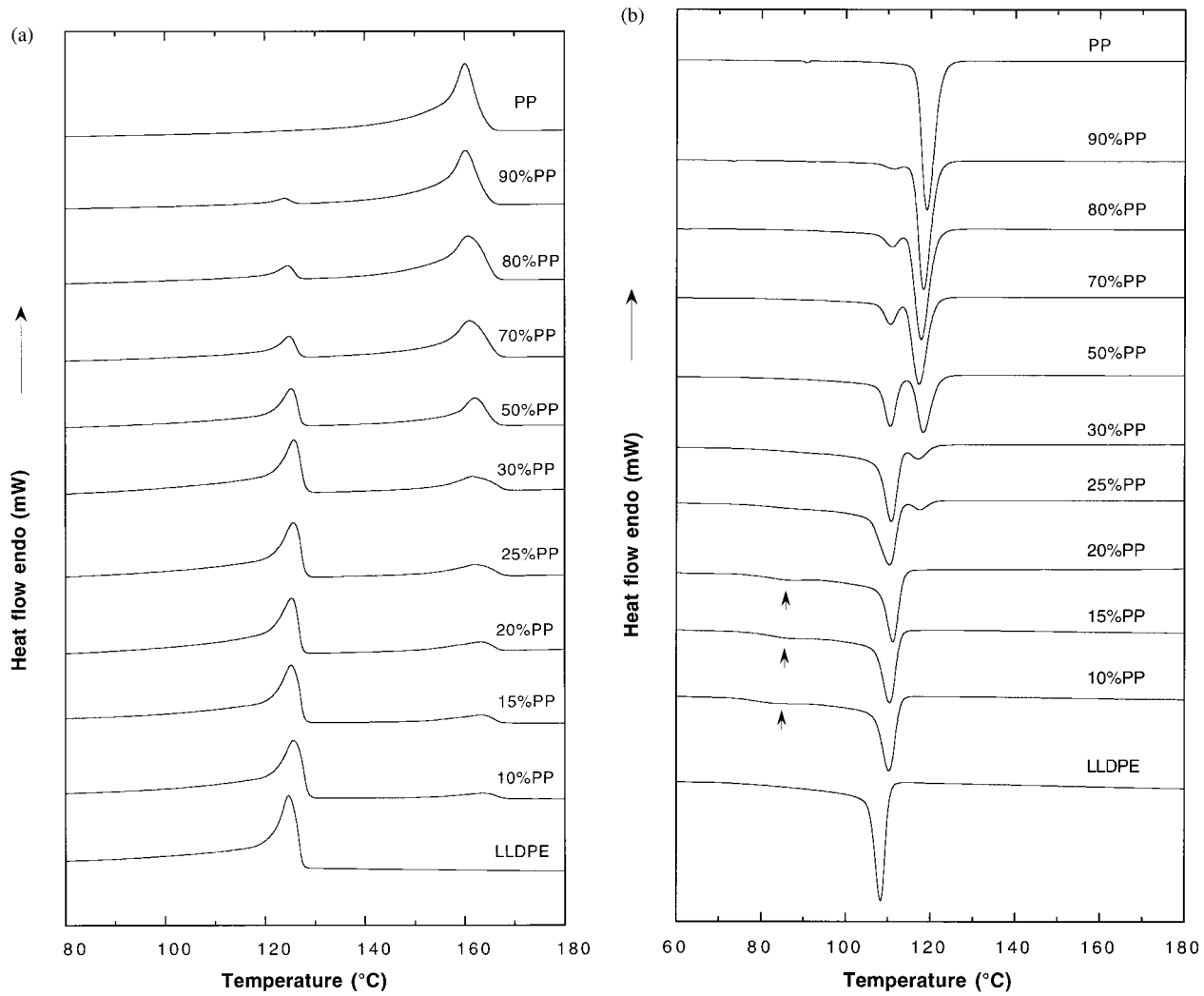

Figure 1 (a) DSC melting curves; (b) DSC cooling curves of PP, LLDPE, and their blends.

performed in bursts of 20 s to a cumulative time of 2 min. A JEOL JSM-35CF SEM with a secondary electron detector was used, operating at 20 kV.

RESULTS AND DISCUSSION

Melting and Crystallization

In the blends, the melting temperature (T_m) of PP increased slightly [Fig. 1(a)]. The increase in the T_m of PP could be caused by the dissolution of defective PP molecules into the LLDPE. It was proposed by Greco et al.[26] that EPR can selectively dissolve defective PP molecules, leaving the more stereoregular PP molecules to form more perfect crystals and a narrower distribution of lamellae or crystalline dimensions in the blends, resulting in a higher T_m. The increased T_m of PP was also observed in the blends of PP with ultralow-density PE (ULDPE)[27] and was attributed to the same reason.

The T_m of LLDPE also changed slightly in the blends [Fig. 1(a)]. However, the degree of change is smaller than that of PP, implying that PP may be more soluble in LLDPE than is LLDPE in PP.

The crystallization endotherms (T_c) of both PP and LLDPE shifted toward each other in the blends [Fig. 1(b)], indicating a mutual interaction. The T_c of LLDPE increased 2–3°C in the blends, while the composition of PP did not affect the T_c of LLDPE significantly. On the contrary, the T_c of PP also decreased slightly with the LLDPE composition to 70%, but its crystallization behavior

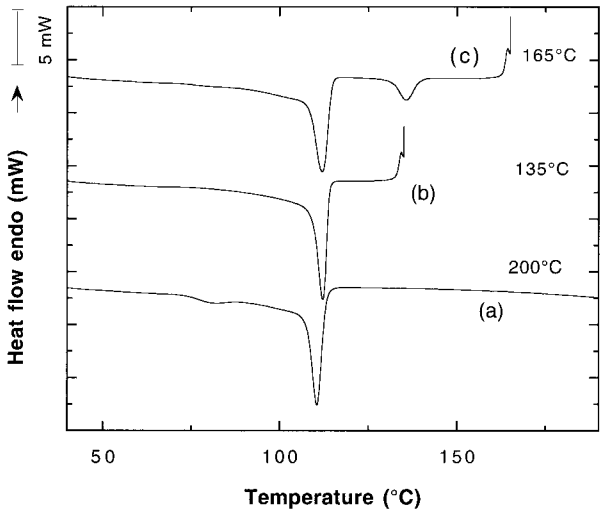

Figure 2 DSC cooling curves of a 20% PP blend after being melted at (a) 200°C, (b) 165°C, and (c) 135°C.

changed radically when the concentration of LLDPE was above 80%.

Small broad crystallization exotherms were observed at approximately 88°C [Fig. 1(b), indicated by arrows] in the 10, 15, and 20% PP blends, whereas the peaks at normal crystallization temperatures of PP (between 117 and 119°C) disappeared. The peak at 88°C may be the crystallization exotherm of PP, although the melting temperature of PP was still at approximately 163°C.

To verify that this small peak was the crystallization exotherm of PP, a melting at lower temperatures and a subsequent cooling experiment was performed. A 20% PP specimen was selected to melt at 135 and 165°C, respectively, for 10 min, followed by cooling to 40°C. Figure 2 shows the DSC cooling curves obtained after melting. The specimen that was melted at 135°C did not show any exotherm at 88°C on cooling [curve (b)], because the crystalline PP should not melt at 135°C and, therefore, no molten PP was available to crystallize upon cooling. This confirmed that the material crystallized at 88°C was the PP, since it did not melt at 135°C. In addition, the crystallization peak of LLDPE shifted to a higher temperature after annealing at 135°C, due to the nucleation effect of the existing PP crystals in the blends.

The specimen that was annealed at 165°C displayed two peaks on cooling (135 and 112°C), corresponding to the T_c of PP and LLDPE, respectively [curve (c) in Fig. 2]. It should be noted that PP crystallized before LLDPE and at a much higher temperature (135°C), compared with 119°C in pure PP. The reason was that a temperature of 165°C was able to melt PP but was not high enough to kill all self-nuclei. The self-nuclei induced the early crystallization of PP in the 20% PP blend. The crystallization of PP at a higher temperature also brought about the highest crystallization temperature for LLDPE, due to the nucleation effect again.

Therefore, it seems that the PP lacked nuclei, so the crystallization was delayed until a lower temperature. PP was also observed to crystallize at an extraordinarily low temperature (50°C) by Pukanszky et al.[28] in a PP (20%)–EPDM (80%) blend after the crystallization peak of EPDM, which was attributed to a different nucleation mechanism. They proposed that, at 20% concentration, PP existed as discrete domains in the PP–EPDM blend. Some droplets were too small and may not contain heterogeneous nuclei, so the crystallization could only start after homogeneous nucleation took place.

Another mechanism for causing lower crystallization of PP can be explained by the Li and Jungnickel's proposal.[29] A compositional change was regarded as the reason for the phase separation in blends of polycaprolactone (PCL) and low molecular weight polystyrene (PS).[29] As PCL and PS were miscible in the melt, when the PCL crystallized, the concentration of PS in the melt increased. Particularly, in the region around the PCL crystals, the concentration of PS was much higher than in other regions. Eventually, the PS droplets appeared at the boundary of growing PCL spherulites and phase separation was induced by the crystallization of PCL. In our system, 20% or less of PP could be dissolved in molten LLDPE. The concentration of PP was highly diluted in these blends and the density of PP segments was not high enough to nucleate at its normal temperature on fast cooling. Only immediately after the LLDPE crystallized did the concentration of PP in the melt increase, especially at the crystallization front of LLDPE, and the PP was able to crystallize after the LLDPE. The crystal solid of LLDPE can act as additional nuclei to promote the crystallization of PP after LLDPE crystallization, that is, the crystallization of PP in the PP–LLDPE blends can be caused by a compositional change, which was the result of miscibility between the PP and the LLDPE. Both mechanisms could operate in the same blend system that we studied and they both suggested that less than 20% of PP was able to dissolve in the molten

Table I Crystallinity (Ratio) of PP and LLDPE in Both the Pure Polymers and in the Blends

Sample	Crystallinity of PP	Crystallinity of LLDPE
PP	0.48	—
90% PP	0.46	0.41
80% PP	0.46	0.42
70% PP	0.46	0.43
50% PP	0.39	0.40
30% PP	0.38	0.40
25% PP	0.37	0.41
20% PP	0.36	0.42
15% PP	0.40	0.42
10% PP	0.36	0.42
LLDPE	—	0.42

LLDPE or, at least, the PP was able to disperse in the LLDPE with very fine particles.

Crystallinity

The crystallinity was calculated based on melting enthalpies. Values of 209 J g^{-1} for PP[30] and 287 J g^{-1} for LLDPE[31] were used for 100% crystallinity.

The crystallinity of PP decreased upon the addition of LLDPE (Table I). A more pronounced decrease occurred when LLDPE was more than 50%, indicating that LLDPE retarded the crystallization of PP, and there was a certain degree of miscibility between PP and LLDPE. On the other hand, the crystallinity of LLDPE was barely affected by the presence of PP. Therefore, it is clear that the effect of LLDPE on PP was more significant than was that of PP on LLDPE.

Equilibrium Melting Temperature

Table II lists the equilibrium melting temperatures (T_m^0) for pure PP and the blends. The T_m^0 PP first increased with the addition of LLDPE and reached the highest temperature (208°C) at 30% of PP, then decreased after PP was 25% or lower in the blends. Even though T_m^0 represents the melting of the equilibrium crystalline state of PP, T_m^0 is a function of blend composition in this case, since the ratio of PE present in the blends influences the equilibrium crystallization of PP. The observed changes in T_m^0 are directly related to the crystal sizes of PP, and PP was able to form the largest crystals in the 30% PP blend.

Table II Equilibrium Melting Temperature (°C) of PP in Pure PP and the Blends

Composition of PP	T_m^0 of PP (°C)
100%	179.3
90%	179.7
80%	182.7
70%	182.4
50%	186.2
30%	208.3
25%	205.5
20%	184.4
15%	173.9
10%	168.9

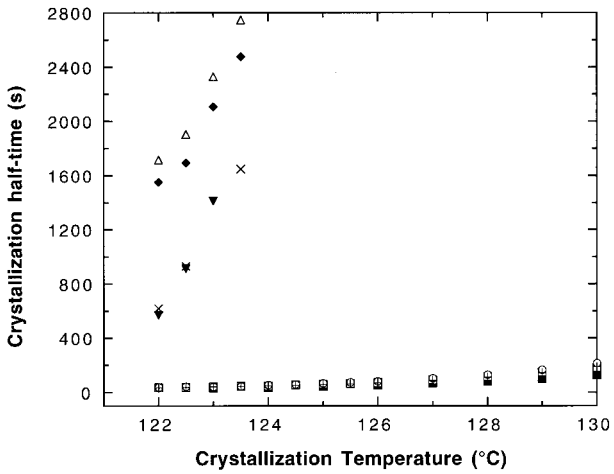

Figure 3 Crystallization half-time of PP versus crystallization temperature for the blends and the pure PP: (■) PP; (▲) 90% PP; (□) 80% PP; (○) 70 % PP; (+) 50% PP; (▼) 30% PP; (×) 25% PP; (♦) 20% PP; (△) 10% PP.

A melting-temperature depression was observed when PP was 10 and 15% in the blends, confirming that the blends of PP–LLDPE with no more than 15% of PP were miscible (Nishi–Wang equation*).[32] A significant decrease in T_m^0 from 205 to 184°C occurred from 25 to 20% of PP in the blends (Table II). This may suggest that the miscibility behavior of PP and LLDPE became favorable at 20% of PP in the blends.

Crystallization Rate

Crystallization Half-time

Figure 3 shows the crystallization half-times versus crystallization temperatures for the pure PP

* $(1/\phi_1)[(1/T_{mb}^0) - (1/T_m{}^0)] = -[(RV_2)/(\Delta H_f V_1)]\,\chi\,\phi_1$, where T_{mb}^0 and T_m^0 are the equilibrium melting temperatures of PP in the blends and pure PP, respectively; ΔH_f, the heat of fusion per mole of crystalline repeat units; V_1 and V_2 , the volumes of the amorphous and crystallizable polymer repeat units; χ, the Flory interaction parameter; and ϕ_1, the volume fraction of a noncrystallizable polymer. Since T_{mb}^0 is smaller than is $T_m{}^0$, χ is negative and, hence, PP was miscible with LLDPE at and below 15% of PP.

Table III Spherulite Growth Rate (nm s^{-1}) of PP in the Pure PP and the Blends

	124°C			126°C			128°C			130°C		
Sample	i	d	g	i	d	g	i	d	g	i	d	g
10% PP			6	29	2	4	21		4	18		2.5
15% PP	33	8	12	31	5	11	23	3	10	22	2	5.4
20% PP												6.2
25% PP	110		48	92		39	65		21	34		18
30% PP												35
50% PP												44
70% PP												61
80% PP												71
90% PP												81
PP												86

i: Initial spherulite growth rate; d: spherulite growth rate during diffusion to LLDPE phase; g: final spherulite growth rate.

and the PP–LLDPE blends. The half-time increased with increasing concentration of LLDPE, and a dramatic increase occurred when the concentration of LLDPE was over 70%.

Spherulite Growth Rate

The growth rate of the PP spherulites decreased with an increase in crystallization temperature and an increasing concentration of LLDPE in the blends (Table III). It changed over a broad range, from 86 nm s^{-1} for the pure PP to 2.5 nm s^{-1} for the 10% PP blend at 130°C.

The decrease of the spherulite growth rate in the blends could be caused by three reasons: The first was that LLDPE acted as a solvent and diluted PP. The concentration of PP in the blends was not high enough to cause nucleation and the crystallization of PP was retarded. The second possibility was that the viscous LLDPE affected the diffusion speed of PP chain segments during crystallization. Finally, the decreased supercooling, which was the result of the miscibility of PP and LLDPE, can reduce the spherulite growth rate. All three reasons suggested that PP was miscible with LLDPE. A detailed discussion on the relationship between the miscibility and the spherulite growth rate was reported separately.[24]

Additionally, in the blends with PP concentrations below 25%, the spherulite growth rate varied with the crystallization time and experienced three different rates, at a given crystallization temperature. Figure 4(a) shows that a plot of the PP spherulitic radius against time is not linear. The growth rate was high initially and then decreased to a very low value. After a period of

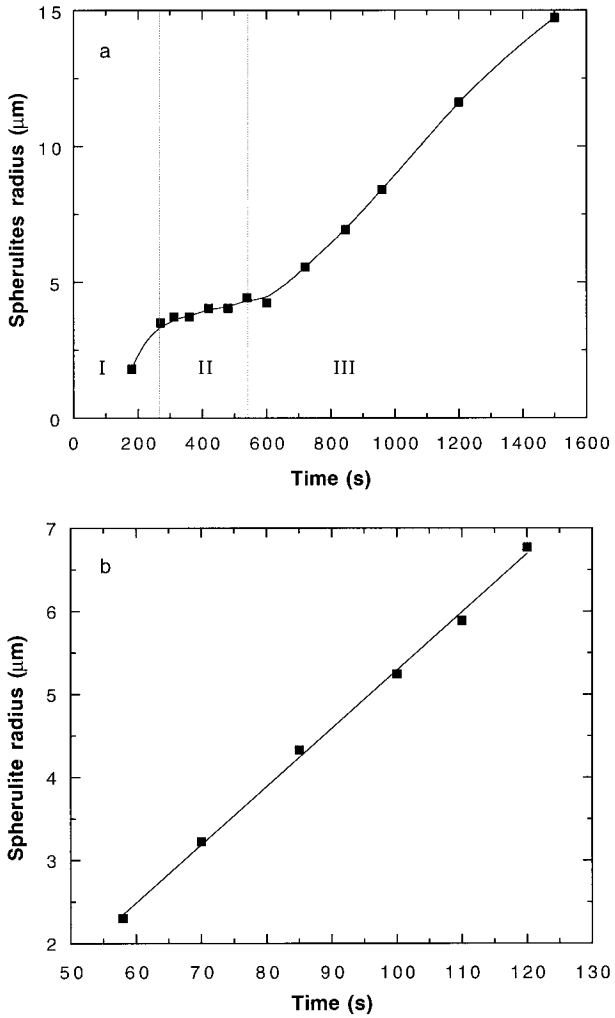

Figure 4 Spherulite radius of PP versus time for (a) a 15% PP blend at 124°C, showing three periods of spherulite growth and (b) a 90% PP blend at 130°C, showing constant growth.

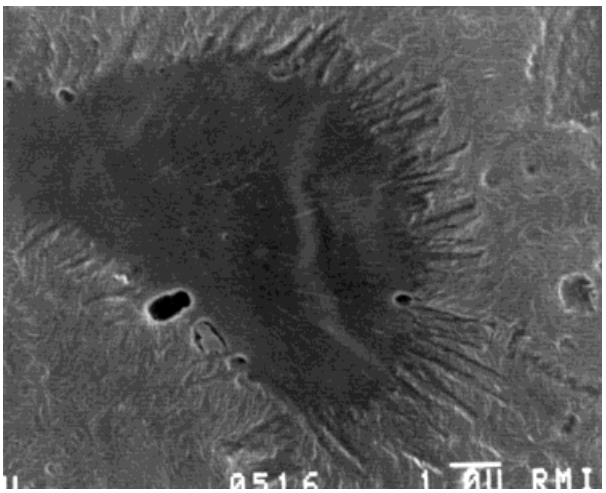

Figure 5 SEM image of a 20% PP blend displaying PP lamellae in the LLDPE phase.

approximately 5 min, the growth rate increased and remained constant thereafter. However, it was still lower than the initial growth rate. For the pure PP and the blends with more than 30% of PP, a plot of the PP spherulite radius against time is linear as shown in Figure 4(b), indicating a constant growth rate.

The growth rates for the three periods can be explained by the miscible behavior between PP and LLDPE. The initial growth rate was high because the PP started to crystallize in a very small volume in its own phase, in which almost 100% of PP was present. The growth rate was close to that of pure PP. After the initial growth, PP had to break through the LLDPE phase for further growth. A certain amount of energy was dissipated during the penetration process from the PP phase to the LLDPE phase, which reduced the growth rate of the spherulites. After the PP grew out of the PP phase into the LLDPE phase, the growth rate increased compared with period II [Fig. 4(b)]. However, it was still lower than the initial growth rate. This was because the PP no longer grew in its own phase and the growth rate was influenced by the viscosity of LLDPE. The breakthrough of PP crystals into the LLDPE phase was observed in the 20% PP blend by SEM (Fig. 5).

Morphology of PP–LLDPE Blends

Spherulite Structure

The observed initial crystallization temperatures for PP and LLDPE under a polarizing microscope with a hot stage were 136 and 119°C, which were detected by the initial appearance of nuclei at a 2°C min^{-1} cooling rate after melting at 200°C for 5 min. Selected isothermal crystallization temperatures were 124, 126, 128, and 130°C. Since these temperatures were above the crystallization temperature of LLDPE, only PP was able to crystallize.

Images (a) and (b) (Fig. 6) show typical spherulitic structures of PP and LLDPE, respectively. Upon the addition of 10% of LLDPE, small droplets appeared in the PP intraspherulitic regions [Fig. 7(a)]. When the amount of LLDPE increased to 20%, the number and size of the droplets increased [Fig. 7(b)]. It can be seen that the LLDPE droplets were engulfed inside the PP spherulites, and the PP was unable to push these droplets to

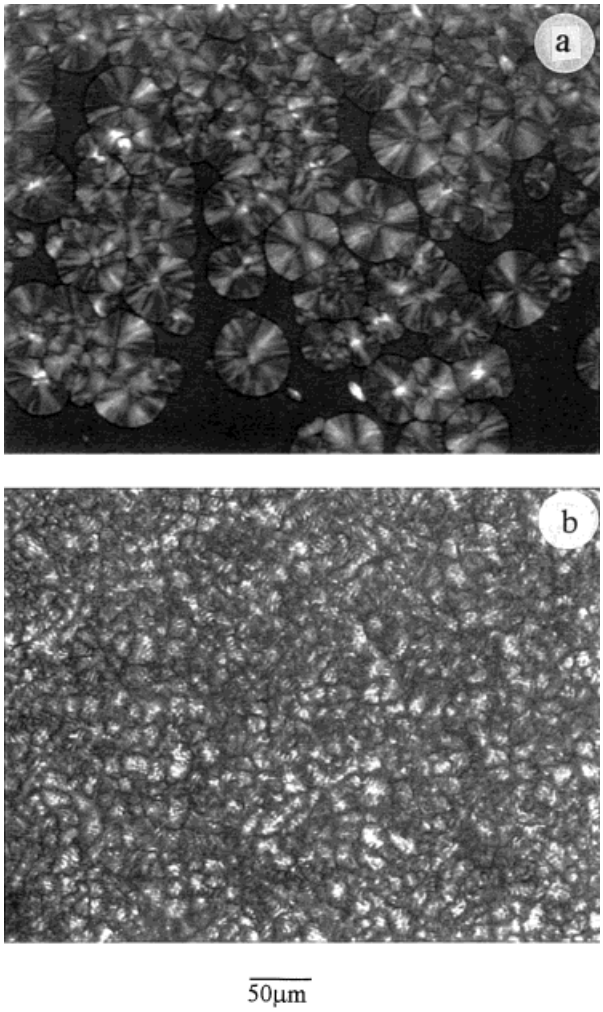

Figure 6 (a) PP spherulites after crystallization at 130°C for 7 min; (b) LLDPE spherulites after crystallization at 130°C for 30 min. Magnification ×100.

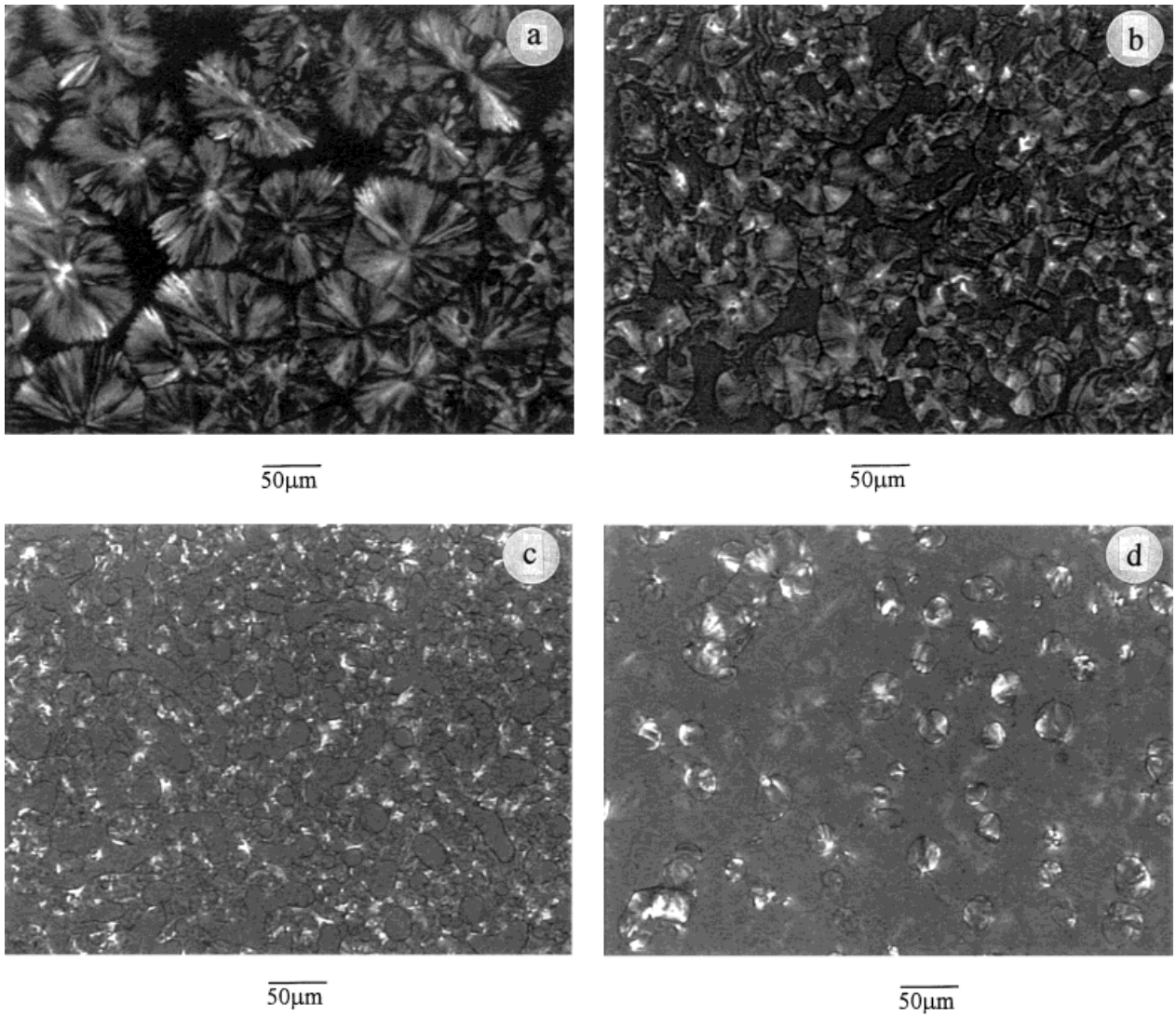

Figure 7 (a) PP spherulites in a 90% PP blend after crystallization at 130°C for 18 h; (b) PP spherulites in an 80% PP blend after crystallization at 130°C for 79 min; (c) cocontinuous morphology in a 70% PP blend after crystallization at 130°C for 17 h; (d) both diffuse PP spherulites and droplets in a 50% PP blend after crystallization at 130°C for 16 h. Magnification ×100.

the interspherulitic region or to deform them, indicating that LLDPE disturbed the crystallization of PP. At 30%, LLDPE became a continuous phase [Fig. 7(c)], forming a co–continuous morphology in the blend. These results differed from previous studies. Dumoulin et al. found co–continuous behavior between 75 and 50% of LLDPE.[9–12] In this work, a co–continuous morphology was found in the range of 30–50% of LLDPE, while LLDPE was the minor component. In the 50% PP blend, it was observed that PP crystallized both from the droplets and from a solution of the melt of PP and LLDPE [Fig. 7(d)] but crystallized mainly in its own separated phase.

PP also crystallized both from droplets and from solution in the 30% PP blend (Fig. 8). Moreover, the droplets of PP were much smaller and the spherulites that crystallized from the solution were still in a small volume. When PP was 25% in the blend [Fig. 9(a)], the droplets of PP became much smaller and they were trying to link together, forming a structure like one of a bunch of grapes. In the 20% PP blend [Fig. 9(b)], the little droplets connected through the lamellar, which was observed by TEM,[33] forming a shape of a spherulite. This lamellar structure was observed to contribute to unique mechanical properties.[34] When the amount of PP was reduced to 15 and

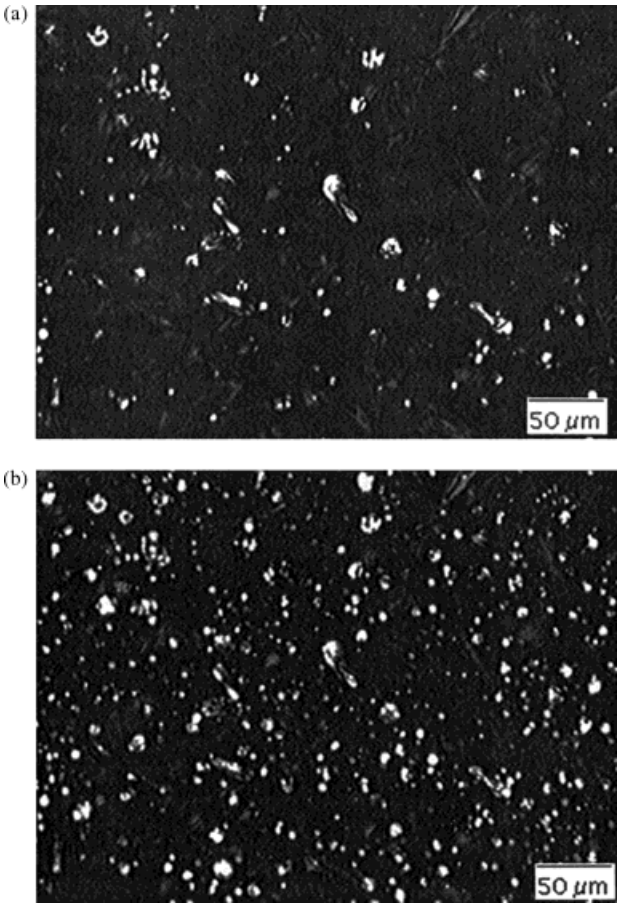

Figure 8 PP droplets and spherulites in a 30% PP blend after crystallization at 130°C for (a) 16 min and (b) 70 min, showing more droplets. Magnification ×100.

10% in the blends, the diffused and imperfect spherulites with needlelike arms were the dominant feature of the crystals [Fig. 9(c,d)]. This kind of crystal structure was also present in the 20% PP blend, although being less in volume.

Relationship Between Morphology and Miscibility

Two distinguished morphologies were observed in the blends with less than 20% and more than 20% of PP. This was caused by different crystallization mechanisms that were, eventually, the result of the miscibility difference of PP–LLDPE blends with variations of the composition ratio.

PP crystallized in a separated phase when its concentration was above 20%, while PP crystallized as open-armed diffuse spherulites in the blends with less than 20% of PP, which are often observed in highly diluted miscible blends such as *isotactic* PP and *atactic* PP blends[35] and PP–EPR blends.[36] With all the above evidence, it can be concluded that the blends of PP–LLDPE with less than 20% of PP were miscible at the crystallization temperatures. The crystallization of PP in these blends was from a homogeneous solution.

The formation of a diffuse spherulitic structure can be explained as follows: During crystallization, PP tended to crystallize on its own, rejecting foreign components. As a large amount of noncrystallizable foreign components (e.g., more than 80% of molten LLDPE) had to be rejected from the growing spherulites, additional energy was consumed. The formation of new lamellae was usually sacrificed in favor of the thickening of the existing lamellae. Therefore, the lamellae were coarser and further apart. The spherulite structure was irregular because the concentration of PP in the matrix was significantly diluted by LLDPE and so the supply of PP was diminished. In contrast, the homopolymer formed compact and symmetric spherulites [Fig. 6(a)]. The coarser lamellae were also the result of decreased supercooling caused by a lower equilibrium melting temperature of PP in the miscible blend.

In the blends with more than 20% of PP, PP crystallized in its own phase, either in a continuous matrix or discrete droplets, depending on the PP composition in the blends. The spherulitic structure in these blends was similar to that of pure PP. It can be seen that each droplet is a single spherulite [Figs. 7(d) and 8]. Such morphologies were the result of the immiscibility of PP–LLDPE blends at these composition ratios.

Relationship Between Miscibility and Crystallization Rate

The decreased overall crystallization rate in the blends was due to the decrease in nuclei density as well as the decrease in spherulite growth rate in the miscible blends.[24] It can be seen from Figures 6 and 7 that the nuclei density was diluted by LLDPE and decreased with the increasing composition of LLDPE. In this study, the significant decrease in the overall crystallization rate in the less than 20% of the PP blends (Fig. 4) was caused predominantly by the drastic decrease in the spherulite growth rate, which was the result of different crystallization mechanisms in these blends.

The crystallization mechanism of PP in the blends with PP concentrations below 20% was different from that in blends with more than 20% of PP. The PP crystallized from a homogeneous solution in the 10 and 15% PP blends [Fig. 9(a,d)], because 15% or less of PP could be dissolved in the

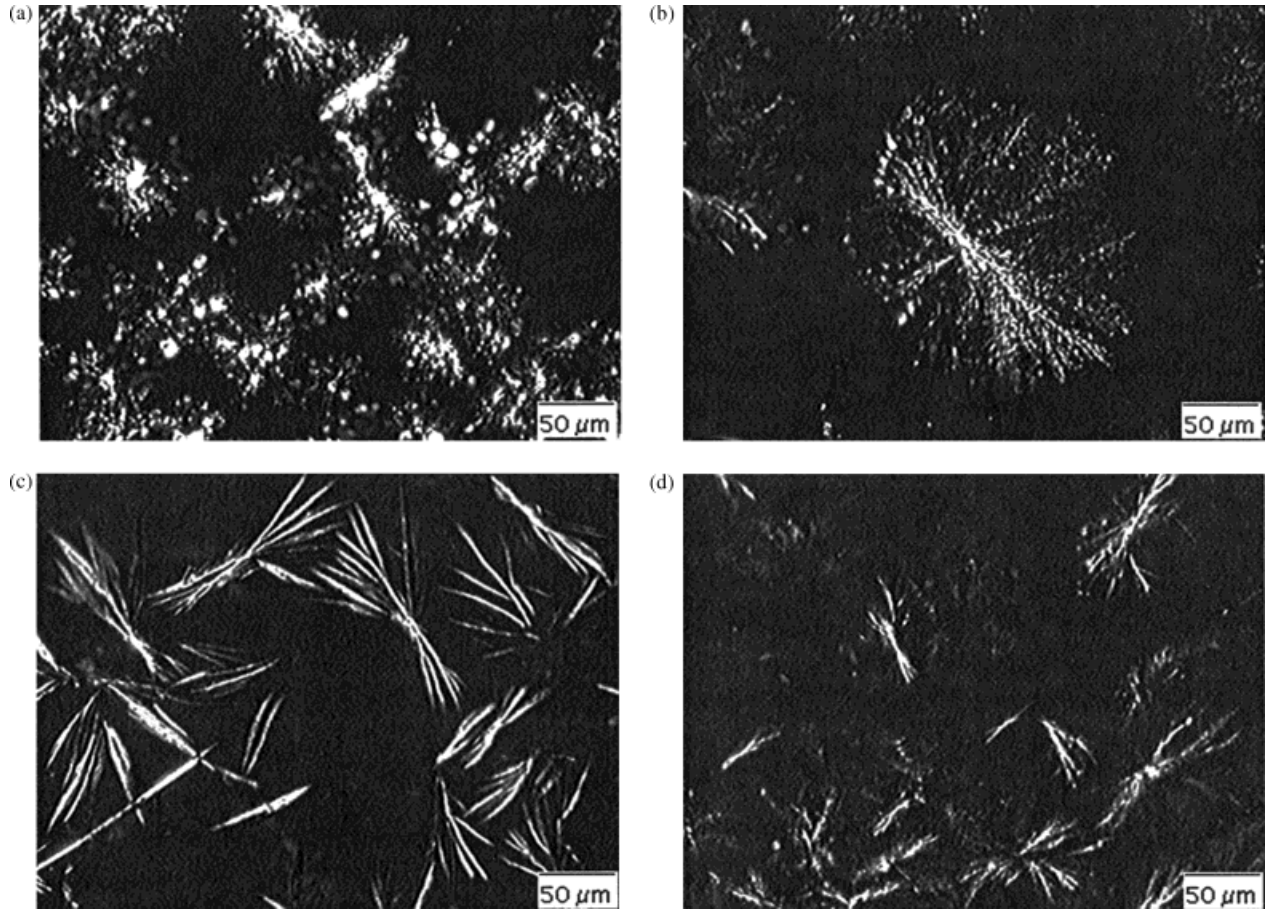

Figure 9 (a) PP droplets in a 25% PP blend after crystallization at 130°C for 61 min; (b) diffuse PP spherulites in a 20% PP blend after crystallization at 130°C for 200 min; (c) sharp PP spherulites in a 15% PP blend after crystallization at 130°C for 160 min; (d) diffuse PP spherulites in a 10% PP blend after crystallization at 130°C for 21 h. Magnification ×100.

LLDPE at the crystallization temperatures. The growth rate of solution-grown spherulites was significantly slower than that of pure PP (Table III), and so was the overall crystallization rate (Fig. 3).

In the blends with 70– 90% of PP, as PP was immiscible with the LLDPE at these concentrations, PP crystallized in a phase-separated major phase (Fig. 7), similar to that in pure PP (Fig. 5). In the blends with 30 and 50% of PP, PP crystallized both in the droplets and in the solution [Figs. 7(d) and 8]. However, crystallization in its own continuous phase was the dominant mechanism in the 50% of PP blend [Fig. 7(d)]. Therefore, the crystallization rate in the 50% PP blend was still close to that of pure PP.

In the 30% PP blend, both droplet and solution-grown crystallization were operating, and it seems that there was a competition between the crystallization and liquid–liquid phase separation. It was observed that, with increase of the crystallization time, the volume of the crystallized droplets increased gradually, at a sacrifice in the concentration of needlelike crystals from the solution. It seems that the droplets were able to suck the dissolved PP from the solution slowly. Images (a) and (b) in Figure 8 are of the same area of the same specimen but recorded at different times. Image (b) shows that more droplets of PP separated from the solution with a longer crystallization time. The slow solution crystallization and gradual transformation from solution-grown crystals to droplets delayed the overall crystallization rate.

It can be concluded that the overall crystallization rate is an indication of the miscibility of PP and LLDPE. The overall crystallization rate was significantly decreased in the miscible blends since the decrease in the spherulite growth rate in these blends is a dominant feature. The overall

crystallization rate was close to that of bulk PP crystallization in the immiscible blends, because the crystallization mechanism in the separated phase was similar to that of bulk crystallization.

CONCLUSIONS

The change in melting and crystallization temperatures of PP and LLDPE indicated that there was some degree of interaction between PP and LLDPE. The decrease of the PP spherulite growth rate in the blends also suggested that PP was partially miscible with LLDPE. The observed equilibrium melting temperature depression in the blends with less than 15% of PP confirmed that PP was miscible with LLDPE at and below 15% of PP. In addition, a significant decrease in T_m^0 from the 25% PP blend to the 20% PP blend suggested that the miscible behavior became favorable when PP was 20%. The optical microscopic images showed that PP crystallized in phase-separated droplets or the matrix in the blends with more than 25% of PP. On the contrary, PP crystallized as open-armed, diffuse spherulites in the blends with 15% or less of PP. These open-armed, diffuse spherulites are often observed in miscible blends. The SEM also showed that PP was able to grow into the LLDPE phase. The significant decrease in the overall crystallization rate in the blends with 20% or less of PP was predominantly caused by a significant decrease in the spherulite growth rate, which was, in turn, caused by the miscibility behavior between PP and LLDPE in these blends.

The authors would like to thank Orica Pty. Ltd. for providing materials. One of the authors (J. L.) acknowledges the receipts of an Overseas Postgraduate Research Scholarship (OPRS) and an Australian Postgraduate Award (APA) at different stages of this project. Special thanks are given by the authors to Dr. Kate Drummond (CRC for Polymers) and Dr. Gandara Amarasinghe for suggestions in the preparation of this manuscript.

REFERENCES

1. Blackadder, D. A.; Richardson, M. J.; Savill, N. G. Macromol Chem 1981, 182, 1271.
2. Noel, O. F.; Carley, J. F. Polym Eng Sci 1984, 24, 488.
3. Wignall, G. D.; Child, H. R.; Samuels, R. J. Polymer 1982, 23, 957.
4. Lohse, D. J. Polym Eng Sci 1986, 26, 1500.
5. Montes, P.; Rafiq, Y. A.; Hill, M. J. Polymer 1998, 39, 6669.
6. Blom, H. P.; Teh, J. W.; Bremner, T.; Rudin, A. Polymer 1998, 39, 4011.
7. Dong, L.; Olley, R. H.; Bassett, D. C. J Mater Sci 1998, 33, 4043.
8. Avalos, F.; Lopez-Manchado, M. A.; Arroyo, M. Polymer 1996, 37, 5681.
9. Dumoulin, M. M.; Farha, C.; Utracki, L. A. Polym Eng Sci 1984, 24, 1319.
10. Dumoulin M. M.; Carreau, P. J. Polym Eng Sci 1987, 27, 1627.
11. Dumoulin, M. M.; Utracki, L. A.; Carreau, P. J. In Two phase Polymer Systems; Utracki, L. A., Ed.; Hanser: Munich, 1991; pp 185–212.
12. Utracki, L. A. ACS Symposium Series 395; American Chemical Society: Washinton, DC, 1989; p 153.
13. Yeh, P. L.; Birley, A. W. Plast Rubb Process Appl 1985, 5, 249.
14. Flaris, V.; Stachurski, Z. H. Polym Int 1992, 27, 267.
15. Flaris, V.; Stachurski, Z. H. J Appl Polym Sci 1992, 45, 1789.
16. Muller, A. J.; Latorre, C.; Mendez, G.; Rotino, J.; Rojas, J. L. ANTEC 1994, 2418.
17. Hill, M. J.; Oiarzabal, L.; Higgins, J. S. Polymer 1994, 35, 3332.
18. Dong, L.; Bassett, D. C.; Olley, R. H. J Macromol Sci-Phys B 1998, 37, 527.
19. Yamaguchi, M.; Miyata, H.; Nitta, K. H. J Appl Polym Sci 1996, 62, 87.
20. Yamaguchi, M.; Nitta, K. H.; Miyata, H. J Appl Polym Sci 1997, 63, 467.
21. Yamaguchi, M.; Miyata, H.; Nitta, K. H. J Polym Sci Phys Ed 1997, 35, 953.
22. Long, Y.; Shanks, R. A.; Stachurski, Z. H. J Mater Sci Lett 1996, 15, 610.
23. Shanks, R. A.; Li, J.; Long, Y. Polymer 2000, 41, 2133.
24. Li, J.; Shanks, R. A.; Long, Y. Polymer 2001, 42, 1941.
25. Avrami, M. J. Chem Phys 1939, 7, 1130; 1940, 8, 21; 1941, 9, 177.
26. Greco, R.; Mancarella, C.; Martuscelli, E.; Ragosta, G.; Jinghua, Y. Polymer 1987, 28, 1929.
27. Lee, Y. K.; Jeong, Y. T.; Kim, K. C.; Jeong, H. M.; Kim, B. K. Polym Eng Sci 1991, 31, 944.
28. Pukanszky, B.; Tudos, F.; Kallo, A.; Bodor, G. Polymer 1989, 30, 1399.
29. Li, Y.; Jungnickel, B. J. Polymer 1993, 34, 459.
30. Aggarwai, S. L. In Polymer Handbook, 2nd ed.; Brandrup, J.; Immergut, E. H., Eds.; 1975; Vol. 24.
31. Quinn, F. A., Jr.; Mandelkern, L. J Am Chem Soc 1958, 80, 3178.
32. Nishi, T.; Wang, T. T. Macromolecules 1975, 8, 909.
33. Li, J.; Shanks, R. A.; Olley, R. H.; Greenway, G. R. Polymer 2001, 42, 7685.
34. Li, J.; Shanks, R. A.; Long, Y. J Appl Polym Sci 2000, 76, 1151.
35. Keith, H. D.; Padden, F. J. J Appl Phys 1964, 35, 1286.
36. Lustiger, A.; Marzinsky, C. N.; Mueller, R. R. J Polym Sci Part B Polym Phys 1998, 36, 2047.